



## Electrochemical and Thermal studies of dipyridotetraaza macrocyclic complexes of Fe (III) and Ni (II)

Sweety\*, Anuj Kumar, Prashant Tevatia and Randhir Singh

Department of Chemistry, Gurukula Kangri Vishwavidyalaya, Haridwar 249404, India

### ABSTRACT

12-membered and 14-membered pyridine based transition metal macrocyclic complexes  $[M^II L^1 Cl_2]$ ,  $[M^{III} L^1 Cl_2]Cl$ , and  $[M^II L^2 Cl_2]$ ,  $[M^{III} L^2 Cl_2]Cl$ , have been synthesized where  $L^1 = 5,6, 11,12$ -tetraphenyl-dipyrido[b, h]1,4,7,10-tetraazacyclododecane and  $L^2 = 5,7,12,14$ -tetramethyl-dipyrido[b, i] 1,4,8,11-tetraazacyclotetradecane.  $M^II = Ni$  (II),  $M^{III} = Fe$  (III). These complexes were characterized by UV-Vis, IR, Mass, TGA/DTA, microanalysis (C, H, and N). These complexes have been assigned saddle-shape nonplanar octahedral configurations on the basis of electronic spectral data. Redox behavior of these macrocyclic complexes were studied by cyclic voltammetric technique. The results suggest quasireversible behavior of most of the redox processes. .

**Keywords:** Macrocyclic complexes, thermal behavior, cyclic voltammetry, diffusion coefficient

### INTRODUCTION

The paramount importance of macrocyclic complexes has been recognized now-a-days. From the past decade, design and synthesis of tetraaza macrocyclic complexes have been widely investigated. The synthetic macrocyclic complexes act as biomimetic models for naturally occurring porphyrin and annulenes [1-5] and received much attention due to their potential applications in catalysis, MRI contrast agents, fuel cell technology, antitumor properties and potency towards DNA binding [6-9]. Polyazamacrocycles resembled to those compounds which are useful as ion selective building block and in catalytic reduction of carbon dioxide [10–11]. The redox potential of macrocyclic complexes tunes over a potential range depending on the nature of donor sites and stereochemical arrangements around metal ions as well as substituents on macrocyclic framework [12]. In this communication synthesis, characterization and cyclic voltammetry of 12 and 14-membered tetraaza macrocyclic complexes of Ni (II), Fe (III) have been carried out. The stabilization of unusual oxidation states and ligand oxidation/reduction has also been observed during electrochemical studies.

### MATERIALS AND METHODS

All chemicals and solvents used were of AR grade. IR spectra were recorded in the 4,000–400  $cm^{-1}$  region with a Shimadzu 8400S spectrometer using KBr DRS system. UV-Vis spectra were recorded on Shimadzu 2450 spectrophotometer in dimethylsulphoxide (DMSO) solvent ( $10^{-4}$  M) solution. The conductivity values were observed on a  $10^{-3}$  mol  $dm^{-3}$  solution in DMF at room temperature by Auto ranging Conductivity/TDS Meter (TCM<sup>+</sup>). Cyclic voltammetry (CV) was performed using an Autolab Potentiostat/Galvanostat 101 instrument with nova software containing three electrode system Pt disc as working electrode, platinum wire as auxiliary electrode, and Ag/AgCl(3M KCl) as reference electrode. Macrocyclic complexes ( $10^{-3}$  M) taken with tetraethylammonium perchlorate (TEAP) (0.1 M) as the supporting electrolyte for experiment. Pre-treatment of electrode and purging of nitrogen were done before running the cyclic voltammograms. Microanalysis and Mass studies (LC-MS) were carried out at CIL SAIF, Punjab University, Chandigarh (Eager Xperience and TOF MS ES+6018e3). TGA/DTA

carried out in CSIR-CBRI Roorkee laboratory on Perkin Elmer Diamond TGA/DTA instrument at a linear heating rate 5<sup>0</sup>/min under nitrogen atmosphere.

**Synthesis of macrocyclic complexes** The macrocyclic complexes were synthesized by template condensation according to literature method [13]

**Synthesis of Dichloro 5,6,11,12-tetraphenyl-dipyrido[b,h]1,4,7,10-tetraazacyclododecane metal [ML<sup>1</sup>Cl<sub>2</sub>] [M=Ni(II)and Fe(III)]**

To a methanolic solution (~20 ml) of 2,3-diamino pyridine (0.244 g, 0.0018 mol) in a round bottom flask was slowly added a methanolic solution (~20 ml) of benzil (0.420g, 0.002 mol) with stirring followed by addition of methanolic solution of metal salts (NiCl<sub>2</sub>.6H<sub>2</sub>O (0.237g, 0.001mol)/anhydrous FeCl<sub>3</sub> (0.162g, 0.001mol) in 2:2:1 molar ratio. The mixture was refluxed for 6 hours, a change in colour was observed. Then the solution was concentrated on rotary evaporator upto dryness washed with methanol and acetone mixture.

**Analytical data:** [Ni(L<sup>1</sup>)Cl<sub>2</sub>](1a) Yield (0.520g, 74 %); m.p. 120 °C; LC-MS spectra showed molecular ion peak at m/z 695, base peak at m/z 624, other peaks are observed at m/z 71, 77, 163,181. [Fe(L<sup>1</sup>)Cl<sub>2</sub>]Cl (1b) Yield (0.695g, 95%), m.p.210 °C; LC-MS spectra of this complex showed peak at m/z 729 corresponding to molecular ion peak, m/z 621 attributed to base peak, other peaks at m/z 182, 106,77, 71, 36 were also observed.

**Synthesis of Dichloro5,7,12,14-tetramethyl-dipyrido[b,i]1,4,8,11-tetraazacyclotetradecane metal [ML<sup>2</sup>Cl<sub>2</sub>] [M=Ni(II), Fe(III)]**

These complexes were synthesized according to above preparation method by using acetyl acetone ((1.00ml, 0.001mol) instead of benzil.

**Analytical data:** [Ni(L<sup>2</sup>)Cl<sub>2</sub>](2a) Yield (0.356g, 73%), m.p. 109 °C; LC-MS: molecular ion peak observed at m/z 475 whereas base peak at m/z 404. others peaks are at m/z, 15, 71,98,165. [Fe(L<sup>2</sup>)Cl<sub>2</sub>]Cl (2b) Yield (0.460g, 90%), m.p.; 140 °C; LC-MS showed molecular ion peak at m/z 507, base peak observed at m/z 401 due to removal of three chloride ion, other peaks at m/z , 256, 71, 36, 15 were also observed.

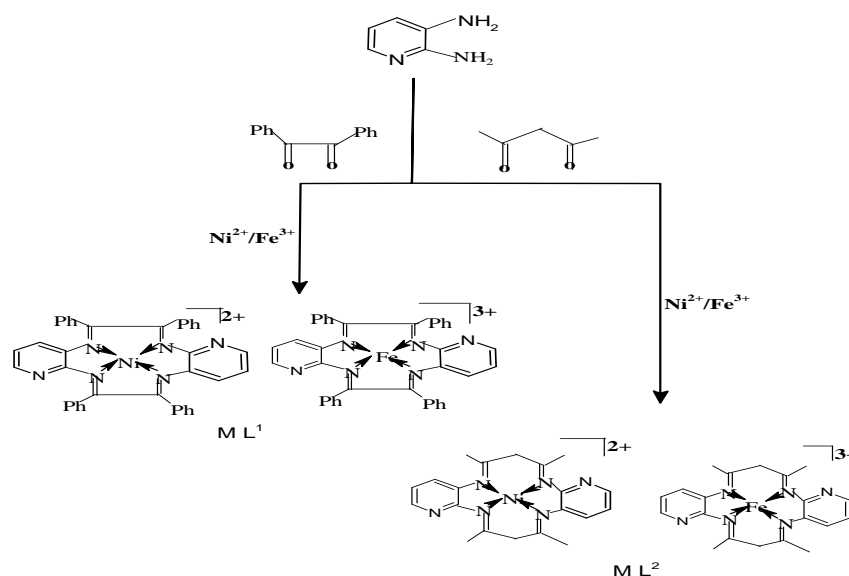


Fig.1 Scheme for synthesis of macrocyclic complexes

## RESULTS AND DISCUSSION

Microanalysis data of these complexes are shown in Table-1. These complexes are stable, non hygroscopic and highly soluble in common solvents. The molar conductivity data in 1mM DMSO corresponds to 1:1 and 1:2 electrolytes for Ni (II) and Fe (III) complexes, respectively.

**Table1: Analytical data, color, melting point and molar conductance of complexes**

Complexes	Color	Mol. Cond.	Microanalysis % found (calculated)		
			C	H	N
[NiC <sub>38</sub> H <sub>26</sub> N <sub>6</sub> Cl <sub>2</sub> ] (695.71)	Dark violet	45	65.52(65.54)	3.70(3.73)	12.01(12.07)
[FeC <sub>38</sub> H <sub>26</sub> N <sub>6</sub> Cl <sub>2</sub> ]Cl (729.84)	Dark yellow	132	62.63(62.65)	3.54(3.56)	11.51(11.50)
[NiC <sub>20</sub> H <sub>22</sub> N <sub>6</sub> Cl <sub>2</sub> ] (475.71)	Dark green	35	50.41(50.45)	4.61(4.62)	17.63(17.65)
[FeC <sub>20</sub> H <sub>22</sub> N <sub>6</sub> Cl <sub>2</sub> ]Cl (507.84)	Brownish yellow	140	47.20(47.25)	4.31(4.33)	16.52(16.54)

**Spectral studies**

IR spectra of these complexes have been observed in the range 400-4000cm<sup>-1</sup>. These macrocyclic complexes showed the absorption bands in the region 416-430 cm<sup>-1</sup> corresponds to  $\nu$  (M-N) stretching vibration. Medium intensity absorption bands appeared in the range of 1590 cm<sup>-1</sup>-1624 cm<sup>-1</sup> due to  $\nu$ (C=N) indicating the formation of macrocyclic framework. The bands at 700-900cm<sup>-1</sup> provide important geometrical information in case of [ML<sup>2</sup>] complex. These bands were assigned to -CH<sub>2</sub> absorptions of macrocyclic framework. The bands at 1577-1600 cm<sup>-1</sup> due to C=C stretching vibration of aromatic ring whereas the bands at 2650-2930 cm<sup>-1</sup> and at 1350-1450 cm<sup>-1</sup> occur due to aromatic C-H stretching and bending vibration of phenyl ring. The band positions and assignments for all the macrocyclic complexes are given in **table 2**.

**Table 2 Vibrational frequencies (cm<sup>-1</sup>) of macrocyclic complexes**

Compound	$\nu$ (M-N)	$\nu$ (C=C)	$\nu$ (C-H)	$\nu$ (C=N)	$\nu$ (-CH <sub>2</sub> )
[NiC <sub>38</sub> H <sub>26</sub> N <sub>6</sub> Cl <sub>2</sub> ]	428	1577	1386	1614	-
[FeC <sub>38</sub> H <sub>26</sub> N <sub>6</sub> Cl <sub>2</sub> ]Cl	435	1590	1410	1600	-
[NiC <sub>20</sub> H <sub>22</sub> N <sub>6</sub> Cl <sub>2</sub> ]	416	1643	1450	1637	735
[FeC <sub>20</sub> H <sub>22</sub> N <sub>6</sub> Cl <sub>2</sub> ]Cl	425	1600	1340	1590	815

The absorption spectra of the Ni (II), Fe (III) complexes have been recorded in DMSO solution at room temperature and data are summarized in **table 3**. The absorption bands observed in the range 200-300 nm indicate  $n \rightarrow \pi^*$  and  $\pi \rightarrow \pi^*$  transitions for all complexes. Ni(II) complexes (1a) and (2a) exhibit bands in the region 360-380 nm corresponding to  ${}^3A_{2g}(F) \rightarrow {}^3T_{2g}(F)$  ( $\nu_1$ ), bands in 420 -425 nm region indicate absorption from  ${}^3A_{2g}(F) \rightarrow {}^3T_{1g}(F)$  ( $\nu_2$ ) and bands in the region 460-515 nm shows absorption from  ${}^3A_{2g}(F) \rightarrow {}^3T_{1g}(F)$  ( $\nu_3$ ). Fe (III) complexes (1b, 2b) exhibit three bands in the region 305-312 nm corresponding to  ${}^6A_{1g}(F) \rightarrow {}^4T_{1g}(F)$  ( $\nu_1$ ), other bands in 405-430 nm range refer to  ${}^6A_{1g}(F) \rightarrow {}^4T_{1g}(P)$  ( $\nu_2$ ) and the band at 470-520 nm are due to  ${}^6A_{1g}(F) \rightarrow {}^4T_{2g}(P)$  ( $\nu_3$ ). The results show that the absorption bands for [ML<sup>1</sup>] complexes are found at lower wavelength due to the presence of phenyl ring on the macrocyclic framework which disturbs the delocalization due to steric hindrance. The Dq (cm<sup>-1</sup>) parameters are calculated by using above transitions [15-16].

**Table 3 Electronic data of macrocyclic complexes**

Compounds	Electronic bands(cm <sup>-1</sup> )	Possible assignment	€(molar extinction coefficients)	Dq (cm <sup>-1</sup> )
[NiC <sub>28</sub> H <sub>22</sub> N <sub>6</sub> Cl <sub>2</sub> ](1a)	360nm(27,778)	${}^3A_{2g}(F) \rightarrow {}^3T_{1g}(P)$	43	2173
	421nm(23,752)	${}^3A_{2g}(F) \rightarrow {}^3T_{1g}(F)$	90	
	460nm(21,739)	${}^3A_{2g}(F) \rightarrow {}^3T_{2g}(F)$	62	
[FeC <sub>28</sub> H <sub>22</sub> N <sub>6</sub> Cl <sub>2</sub> ]Cl(1b)	305nm(32,786)	${}^6A_{1g} \rightarrow {}^4T_{1g}(F)$	65	-----
	415nm(24,096)	${}^6A_{1g} \rightarrow {}^4T_{1g}(P)$	80	
	477nm(20,964)	${}^6A_{1g} \rightarrow {}^4T_{2g}(P)$	33	
[NiC <sub>20</sub> H <sub>22</sub> N <sub>6</sub> Cl <sub>2</sub> ](2a)	380nm(27,777)	${}^3A_{2g}(F) \rightarrow {}^3T_{1g}(P)$	30	1626
	435nm(19,047)	${}^3A_{2g}(F) \rightarrow {}^3T_{1g}(F)$	54	
	510nm(16,260)	${}^3A_{2g}(F) \rightarrow {}^3T_{2g}(F)$	67	
[FeC <sub>20</sub> H <sub>22</sub> N <sub>6</sub> Cl <sub>2</sub> ]Cl(2b)	312nm(32,786)	${}^6A_{1g} \rightarrow {}^4T_{1g}(F)$	23	-----
	428nm(23,255)	${}^6A_{1g} \rightarrow {}^4T_{1g}(P)$	27	
	515nm(20,080)	${}^6A_{1g} \rightarrow {}^4T_{2g}(P)$	58	

### TGA/DTA analysis

Thermo gravimetric analysis (TGA) involves the measurement of mass loss vs temperature which indicates the thermal stability of macrocyclic complexes. Differential thermal analysis (DTA) gives information about the nature of thermal change. The TGA/DTA analysis of the complexes carried out in the temperature range 25-600°C at constant heating rate of 5°/minute. The thermo analytical data are given in **tables 4**. The complex (**1a**) **fig.2** thermogram showed 8 % weight loss from 38- 78° C due to removal of adsorbed solvent molecules with an endothermic peak. Another weight loss 10% in temperature range 80-300°C is due to loss of axially coordinated chlorine molecules with a small exothermic peak. About 30% weight loss occurs up to 420°C with a sharp exothermic peak due to loss of macrocyclic moiety. Complex (**1b**) thermogram showed a weight loss of 4% at 150- 265°C which corresponds to the loss of an outer chloride with an exothermic peak. Another weight loss of 10.20 % found in the range 300-320°C, is due to loss of two axially coordinated chlorides with a sharp exothermic peak. The total mass loss upto 552°C is found to be 90.3%, the remaining mass corresponding to residual metal oxide.

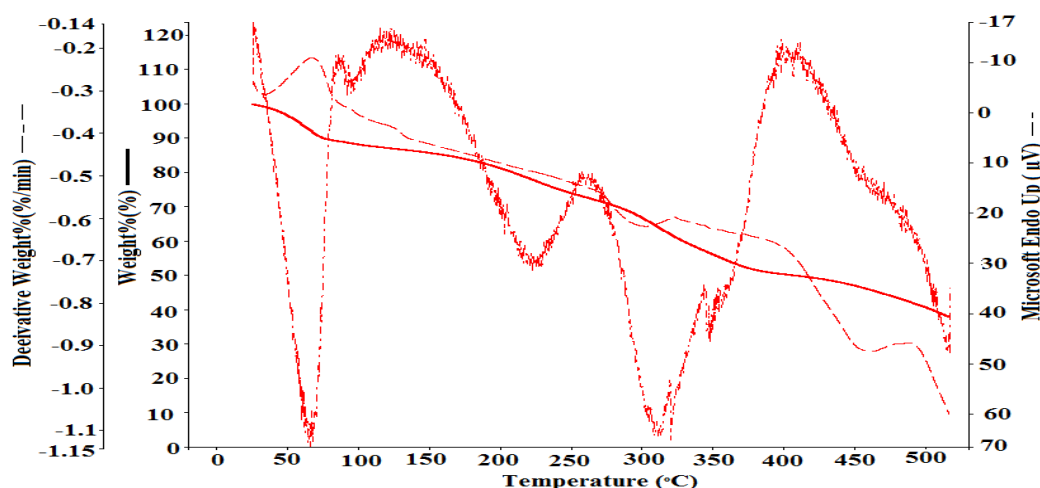


Fig.2 TGA/DTG/DTA curves of complex 1a

Complex **2a** thermogram showed 3% weight loss up to 54°C with a small endothermic peak due to removal of adsorbed solvent molecules, 15% weight loss in temperature range from 100°C to 210°C with two endothermic peaks may be due to coordinated chloride ions. Approximately 20 % weight loss found in the temperature range 240°C to 320°C with endothermic peak due to removal of macrocyclic moiety. Complex **2b** showed a small plateau upto 200°C with an endothermic sharp peak attributed to the 7% weight loss due to removal of chloride ion outside the coordination sphere. About 13% weight loss observed due to axially coordinated chlorine. Further there is no decomposition upto 600°C showing extra thermal stability for this complex [17-18].

Table 4 Thermal behavior data under 1 ml N<sub>2</sub> pressure for macrocyclic complexes

Comp.	Temp. range	Thermal effect	Δm%(exp./calc.)	Probable assignment
[NiL <sup>1</sup> Cl <sub>2</sub> ] ( <i>1a</i> )	38- 78°C	Endothermic	8(---)	Loss of adsorbed solvent molecule
	80-300°C	Exothermic	10(10.43)	Loss of chloride molecule
	upto 420°C	Exothermic	30 (32)	Loss of macrocyclic moiety
[FeL <sup>1</sup> Cl <sub>2</sub> ]Cl ( <i>1b</i> )	150- 265°C	Exothermic	4.70(4.84)	Loss of chloride outside the coordination sphere
	300-320°C	Exothermic	10(10.20)	Loss of axially chloride molecule
[NiL <sup>2</sup> Cl <sub>2</sub> ] ( <i>2a</i> )	upto 54°C	Endothermic	3(---)	Removal of adsorbed solvent molecule
	56- 210°C	Endothermic	15( 16)	Removal of chloride molecule
	220-310°C	Endothermic	20 (20.63)	Loss of macrocyclic moiety
[FeL <sup>2</sup> Cl <sub>2</sub> ]Cl ( <i>2b</i> )	200°C	Exothermic	7 % (6.5)	Loss of chloride outside the coordination sphere
	210-370°C	Exothermic	12(13)	Loss of axially chloride molecule
	Upto 400°C	Endothermic	37(38.67)	Loss of macrocyclic moiety

### Electrochemical studies

The redox properties of all complexes were studied by cyclic voltammetry using Pt electrode (0.031cm<sup>2</sup>) in DMSO containing 10<sup>-3</sup> M complex and 0.1M TEAP. The results obtained are listed in **Table 5**. Cyclic Voltammogram of Ni complex [ML<sup>1</sup>Cl<sub>2</sub>] (**1a**) was recorded in the -2.0 to +2.0 V potential range vs Ag/AgCl under N<sub>2</sub> atmosphere at scan rate of 200 mVs<sup>-1</sup> shown in **fig.3a**. The cyclic voltammogram showed an intense cathodic peak at -0.50 V and on reverse scanning an anodic peak of nearly equal intensity at -0.28 V. The voltammetric parameters, peak separation (ΔE= 0.22 V) and peak current ratio ( $i_{pa}/i_{pc} = 1.01$ ) indicate the corresponding two electron quasireversible Ni (II)

/Ni (0) redox process. Higher value of peak separation ( $\Delta E$ ) for Ni (II)/Ni (0) process may be due to the resistance in the cell solution [19]. Another cathodic peak appeared at potential +0.26 V which can be assigned for Ni (II)/ Ni (I) reduction process. Moreover, the cyclic voltammogram showed a reversible redox couple at potential +1.10 V due to the  $L/L^+$  redox process. The experiment also performed in the -1.0 V to +1.0 V potential region vs Ag/AgCl in the similar condition which shows Ni(II)/Ni(0) redox couple with slight shift in the positive potential region of redox couple may be due to the decrease in the solution resistance whereas the peak current magnitude for this couple is nearly similar. The specific redox couple showed the stabilization of unusual oxidation state. The cyclic voltammogram of Ni complex  $[ML^2Cl_2]$  (**2a**) shown in **fig.3b**, recorded in similar condition which showed an anodic peak at -0.35 V while on reverse scanning a cathodic peak also appeared at -0.46 V. On the basis of peak separation ( $\Delta E=0.11$  V) and peak ratio ( $i_{pa}/i_{pc} = 1.01$ ), the corresponding redox couple can be attributed to quassireversible Ni (II) / Ni (0) redox process. Another redox couple at  $E_{pa} = +0.89$  V and  $E_{pc} = +0.75$  V, showed Ni (II) / Ni (III) redox process. A cathodic peak was also observed at +0.22 V which can be attributed to Ni (II) / Ni (I) reduction process.

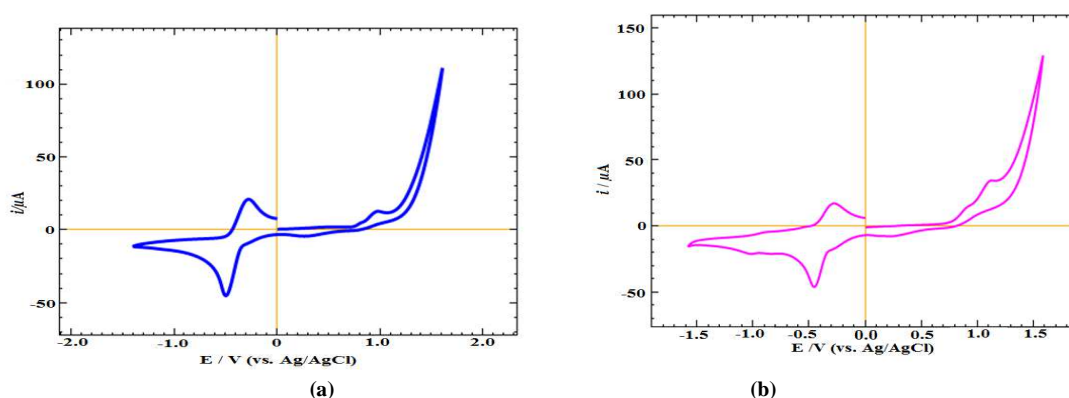


Fig. 3 Cyclic voltammograms (a) 1a complex and (b) 2a complex in DMSO with 0.1M TEAP as supporting electrolyte using a Pt working electrode at a scan rate of  $0.2 \text{ V s}^{-1}$

Cyclic voltammogram of  $[FeL^1Cl_2]$  (**1b**) macrocyclic complex was recorded in DMSO in similar condition in the - 2.0 V to +2.0 V potential range vs Ag/AgCl in **fig.3c**. The observed cyclic voltammogram showed a cathodic peak observed at -1.19 V while on reverse scanning an intense anodic peak at -0.82 V. The corresponding redox couple with the formal potential  $E_{1/2} = -0.99\text{V}$  can be assigned to irreversible redox process Fe (II)/Fe (0). There is another redox process corresponding to anodic and cathodic peaks at -0.61 and -0.32 V which can be attributed to Fe (III)/Fe (II) redox process. An additional cathodic peak at +0.02 V assigned to Fe (II)/Fe (I) reduction process. Similarly, the cyclic voltammogram of  $[FeL^2Cl_2]$  (**2b**) (**Fig. 3d**) showed cathodic and anodic peak potentials at - 1.40V, -1.09V with the peak separation  $\Delta E = -0.31$  showing completely irreversible Fe (II)/Fe (0) redox couple. Another redox couple appeared with peak separation  $\Delta E = -0.20$  V due to Fe (III)/Fe (II) redox process. A cathodic peak observed nearly at +0.87 V due to Fe (II)/Fe (I) reduction.

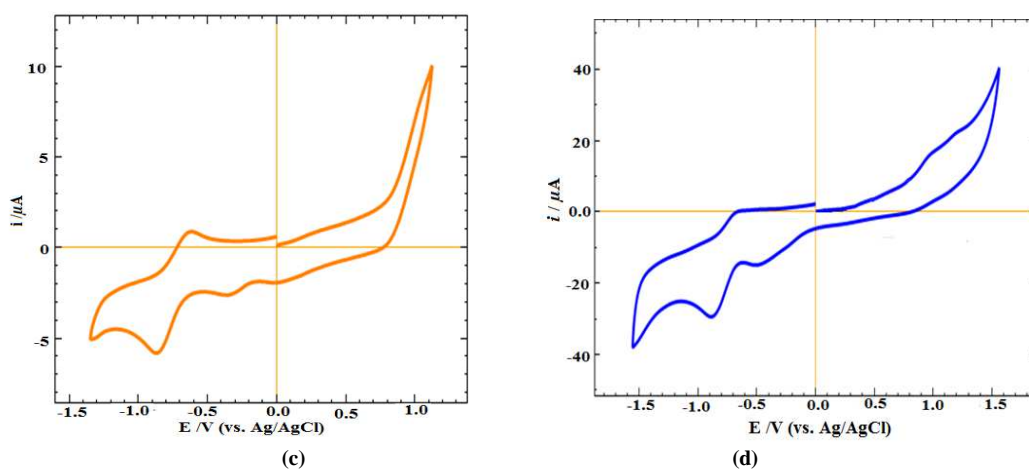


Fig. 3 Cyclic voltammograms (c) 1b complex and (d) 2b complex in DMSO with 0.1M TEAP as supporting electrolyte using a Pt working electrode at a scan rate of  $0.2 \text{ Vs}^{-1}$

The considerable difference between positions of redox couples for macrocyclic complexes (1a) and (2a) and redox couples for macrocyclic complexes (1b) and (2b) can be explained on the basis of effect of substituents. The

presence of four phenyl groups in the (1a) and (1b) macrocyclic framework greatly affects the metal nitrogen bond length due to steric hindrance as a result of which both redox couple shifts slightly towards the positive potential range. The variation in the redox potentials for these redox processes is further supported by UV-Vis absorption shifting. UV-Vis spectra for both macrocyclic complexes (1a) and (1b) showed a blue shift. Macrocyclic ring size also affects the redox potential. As the ring size increases in (2a) and (2b) complexes, metal-donor bond length also increases due to which the redox changes Ni(III) → Ni(II) → Ni(I) occur easily [20]. The same effect is also observed in macrocyclic complex (2b) in which  $E_{1/2}$  value for Fe (II)/Fe (0) redox couple shifted towards positive potential region as compared to (1b) macrocyclic complex due to bigger macrocyclic ring size [21-22].

In order to check the reversible behavior of macrocyclic complexes, cyclic voltammetry experiments were carried out between +0.2 V to -0.2 V at various scan rates. As illustrated in Fig. 4, cyclic voltammogram of 1a shows increase in peak current with increasing scan rate but the ratio of peak currents of anodic and cathodic reactions are almost constant at different scan rates. The peak separation between the corresponding anodic and cathodic peaks increases with increasing scan rate which indicates the fast electron transfer process [23].

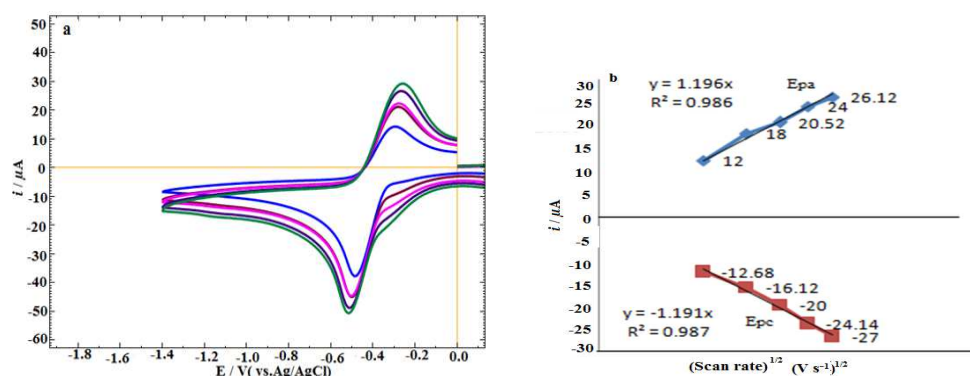


Fig. 4 Cyclic voltammograms (a) of 1a complex in DMSO at scan rate 50-300 V s<sup>-1</sup> and (b) plot of oxidation and reduction peak currents versus square root of scan rate

The heterogeneous electron transfer rate constants for all the macrocyclic complexes were calculated using the Nicolson and Kochi method (Eq.1) and the diffusion coefficients were also calculated by Randles-Sevcik relationship (Eq.2),

$$i_p = 0.227 nF A C K^0 \exp\{-an_a f(E_p - E^f)\} \quad (1)$$

$$i_p = -0.4463nF A (nFD\nu/RT)^{1/2} C \quad (2)$$

Where,  $i_p$  = Peak current ( $\mu A$ ),  $n$  = No. of electron involving in the process,  $F$  = Faraday constant,  $A$  = Area of the electrode,  $C$  = Concentration of the electro active species (mM),  $an_a = 0.048/E_p - E_{p/2}$ , Where,  $E_{p/2} = E_{1/2} - 1.09RT/nF$  [24-25]

Table 5 Electrochemical data of 10<sup>-3</sup> M solution of macrocyclic complexes recorded in DMSO solution at room temperature with reference to Ag/AgCl electrode using (Et<sub>3</sub>N)ClO<sub>4</sub> supporting electrolyte

Compounds	$E_{pa}$ (V)	$E_{pc}$ (V)	$\Delta E$ (V)	$E_{1/2}$ (V)	$D$ (10 <sup>-5</sup> ) cm <sup>2</sup> /s	$k^0$ (10 <sup>-6</sup> ) cm/s	$i_{pa}/i_{pc}$
[NiL <sup>1</sup> Cl <sub>2</sub> ] (1a)	-0.28	-0.50	0.22	-0.39	4.12	2.38	1.01
[FeL <sup>1</sup> Cl <sub>2</sub> ]Cl (1b)	-0.82	-1.19	0.37	-1.0	1.19	1.73	1.5
[NiL <sup>2</sup> Cl <sub>2</sub> ] (2a)	-0.35	-0.46	0.11	-0.87	2.33	2.87	1.00
[FeL <sup>2</sup> Cl <sub>2</sub> ]Cl (2b)	-1.09	-1.40	0.31	-1.2	2.51	3.12	1.7

## CONCLUSION

On the basis of electrochemical findings a comprehensive redox mechanism has been proposed which provide important insights about these biologically important macrocyclic complexes. Electrochemical studies showed the affect of phenyl group and ring size on redox potential of macrocyclic complexes. Thermal studies show ~ 90% weight loss upto 550°C of complexes showing the formation of metal oxides as residue. Thermal decomposition of macrocyclic complexes shows the presence of adsorbed solvent molecule, the composition and also the thermal stability. The results are in good agreement with the composition of complexes. On the basis of the above studies these complexes possess distorted octahedral saddle shape geometry.

**Acknowledgement**

The authors are thankful to CSIR / UGC New Delhi for financial support in the past projects and support is also acknowledged for completing of these studies from SAIF Panjab University Chandigarh and CSIR-CBRI research laboratory, Roorkee.

**REFERENCES**

- [1] G. Ferraudi, J.C. Canales, B. Kharisov, J. Costamagna, J. G. Zagal, *J. Coord. Chem.*, **2005**, 58, 89.
- [2] N. Fahmi, I. Masih, K. Soni, *J. Macromol. Sci. Part A: Pure and Appl. Chem.*, **2015**, 52, 548.
- [3] S. Najlaa, M. Sawsan, A. Ashqar, M.M. Mostafa, *J. Incl. Phenom. Macrocycl. Chem.*, **2011**, 69,157.
- [4] S. Zhan, Y. Miao, L. Ping, C. Yuan, *Trans. Met. Chem.*, **1999**, 24, 311.
- [5] L. Dunbar, R. J. Sowden, K. D. Trotter, M. K. Taylor, D. Smith, *Biomet.*, **2015**, 28, 903.
- [6] Z. P. Li, B. H. Liu, *J. Appl. Electrochem.*, **2010**, 40, 475.
- [7] C.L. Ferreira, D.T.T. Yapp, D. Mandel, R.K. Gill, E. Boros, M. Q. Wong, *Bioconj. Chem.*, **2012**, 23, 2239.
- [8] J. Huang, Q.D. Huang, J. Zhang, L.H. Zhou, L.L. Qiang, N. Jiang, H.H. Lin, W. Jiang, *Int. J. Mol. Sci.*, **2007**, 8, 606.
- [9] P. Zeng, H. Limin, Z. Zhenfeng, N. Yang, Y. Song, *Trans.Met.Chem.* **2015**, 40, 779.
- [10] A. Chaudhary, R.V. Singh, *Russ. J. Chem.*, **2008**, 1, 1.
- [11] V. U. Kamble, A. S. Patil, S. P. Badami, *J. Incl. Phenom. Macrocycl. Chem.*, **2010**, 68, 347.
- [12] J. M. Michael, N, J. Rose, *Inorg. Chem.*, **1984**, 23, 2252.
- [13] N. Raman, C. Thangaraja, *Trans. Met. Chem*, **2005**, 30, 317.
- [14] R. Benramdane, F. Benghanem, A. Ourari, S. Keraghe, G. Bouet, *J. Coord. Chem.*, **2015**, 68, 560.
- [15] W. U. Malik, R. Bembi, R. Singh, *Trans. Met. Chem.*, **1983**, 8, 321.
- [16] R. Olar, M. Badea, D. Marinescu, E. Frunza, E.E. Iorgulescu, *J. Therm. Anal. Calorim.*, **2010**, 99, 815.
- [17] F. Firdaus, K. Fatma, M. Azam, M. Shakir, *J. Coord. Chem.*, **2010**, 63, 3956.
- [18] Y.U. Manawadevi, Y. Liu, C. Forsyth, A.M. Bond, *Trans. Met. Chem.*, **2014**, 39, 883.
- [19] V. L. Frank, E.S. Gore, D.H. Bush, *J. Am. Chem. Soc.*, **1974**, 96, 3109.
- [20] L.O. Spreer, D.B. Macqueen, C.B. Allan, J.W. Otvos, M. Calvin, *Inorg. Chem.*, **1994**, 33, 1753.
- [21] V. L. Goedkin, S.M. Peng, *J. Am. Chem. Soc.*, **1974**, 7693.
- [22] M. I. Bazanov, O. V. Balakireva, A. E. Balakirev, M. V. Kurach, V. E. Maizlish, *Russ. J. Electrochem.*, **2002**, 38, 1000.
- [23] D.C. Alwisa, J. A. Craystona, T. Cromiea, T. Eisenblätte, *Electrochim. Acta.*, **2000**, 45, 2061.
- [24] N. S. Neghmouche, T. Lanez, *Int. J. Chem. Stud.*, **2013**, 1, 28.
- [25] J.C. Dabrowiak, D. P. Fisher, F. C. McElroy, *Inorg. Chem.*, **1979**, 18, 2304.